Available online at www.sciencedirect.com
SCIENCE DIRECT®
Thin Solid Films 447–448 (2004) 449–454
thin solid films
www.elsevier.com/locate/tsf

Structural, optical and mechanical properties of coloured TiN_xO_y thin films

F. Vaz[a,*], P. Cerqueira[a], L. Rebouta[a], S.M.C. Nascimento[a], E. Alves[b], Ph. Goudeau[c], J.P. Rivière[c], K. Pischow[d], J. de Rijk[d]

[a]*Departamento de Física, Universidade do Minho, Azurém, 4800-058 Guimarães, Portugal*
[b]*ITN, Departamento de Física, E.N.10, 2685 Sacavém, Portugal*
[c]*Laboratoire de Métallurgie Physique, Université de Poitiers, 86960 Futuroscope, France*
[d]*Savcor Coatings Oy, Insinöörinkatu 7, FIN-50100 Mikkeli, Finland*

Abstract

Within the frame of this work, coloured films based on single layered titanium oxynitride (TiN_xO_y) compounds were prepared. The films were deposited by r.f. magnetron sputtering under variation of process parameters such as bias voltage and flow rate of reactive gases. Colour varied from shiny golden type for low oxygen contents (characteristic of TiN films) to dark blue for higher oxygen contents. The information on the composition was obtained by Rutherford backscattering spectrometry. X-ray diffraction results revealed the development of a face-centred cubic phase with ⟨1 1 1⟩ orientation (TiN type; lattice parameter of ~0.429 nm) and traces of dispersed oxide phases. Nanoindentation experiments showed values of hardness between 20 and 40 GPa, strongly dependent on the composition and microstructure. Compressive stresses between −0.5 and −6 GPa were determined by the deflection method.

Keywords: Structural properties; Mechanical properties; Optical properties; Sputtering; Ion bombardment; Titanium nitride

1. Introduction

Modern science is fundamental to satisfy the steadily increasing demands of the society for new and high-quality products. In this respect, coloured films are needed for consumer products, such as eyeglass frames, wristwatch casings and wristbands and several jewellery parts. While enhancing the appearance and lending the surfaces attractive colorations the films are supposed to provide scratch-resistance and protection against corrosion.

Regarding the apparent coloration of thin films, one must distinguish between the inherent coloration (e.g. in nitrides, carbonitrides or borides) and apparent coloration due to interference effects (e.g. transparent oxide or ultra-thin absorbing films) [1]. Transition metal nitride coatings (TiN, CrN, WN, ZrN among others) are known for their remarkable mechanical properties, such as high hardness, good wear- and corrosion resistance and adhesion, which make them attractive for tribological applications. At the same time, these materials (e.g. TiN) reveal an intrinsic golden colour, which make them good candidates for decorative application. On the other hand, the apparent coloration of interference films (TiO_2, ZrO_2, among others) is primarily influenced by thickness [2], and thus its use is less suitable as decorative coatings.

Furthermore, the increasing demands for low-cost products and reduced material resources imply that the continuous change in target materials to obtain different coloured films is clearly non-suitable. Taking into consideration that the colour of a certain material (inherent colour) is due to their free electrons from higher wavelengths down to visible region, where they are determined by the selective absorption beginning at these short wavelengths [3], a new class of materials is gaining importance for these decorative applications, the so-called metal oxynitrides, MeN_xO_y (Me = early transition metal).

*Corresponding author. Tel.: +351-253510471; fax: +351-253510461.
E-mail address: fvaz@fisica.uminho.pt (F. Vaz).

0040-6090/04/$ - see front matter © 2003 Elsevier Science B.V. All rights reserved.
doi:10.1016/S0040-6090(03)01123-4

Despite the huge amount of published scientific work on thin films of metallic nitrides and oxides over the last 20 years [1], the area of metal oxynitrides is poorly explored so far. To our knowledge and as it is clear from the published works [1–3], the understanding of the fundamental mechanism that explain both structural and mechanical behaviour is yet insufficient. In fact, a basic understanding of the gas-phase and thin-film oxygen and nitrogen incorporation chemistries facilitates the processing of oxynitride and carbonitrides nanostructures with desirable properties. Taking this into consideration, the main purpose of this work consists on the study of the structural, optical and mechanical properties of coloured TiN_xO_y films as a function of gas mixture.

2. Experimental details

The TiN_xO_y samples were deposited by reactive r.f. magnetron sputtering from a high purity Ti target (99.731%) onto polished high-speed steel (AISI M2), stainless steel, single crystalline silicon (1 0 0) and glass substrates. Prior to all depositions, the substrates were ultrasonically cleaned and sputter etched for 15 min in a 0.4 Pa Ar atmosphere (200 W r.f. power). Depositions were carried out under an Ar/N_2+O_2 atmosphere in an Alcatel SCM650 apparatus, and the substrates were rotating at 60 mm over the target at a constant speed of 4 rpm. The base pressure in the deposition chamber was approximately 10^{-4} Pa and rose to values of approximately 4×10^{-1} Pa during depositions. A pure titanium adhesion layer (600 W r.f. power in Ti target, substrate temperature, T_s, of 300 °C and −50 V bias voltage), with a thickness of approximately 0.30 μm, was deposited in each sample in order to improve the adhesion of the films to the substrates. Substrates were heated up to $T_s=300$ °C and d.c. biased from −50 V up to grounded state. Films were prepared with variation of the gas mixture (N_2+O_2) flux, using constant values of temperature (300 °C) and bias voltage (−50 V). Fluxes varied from 3.3 to 16 sccm, with a partial pressure ranging from 0.02 to 0.05 Pa. The working gas flow (argon) was kept constant at 100 sccm.

The atomic composition of the samples was measured by Rutherford backscattering spectrometry (RBS). An average number of five 'ball cratering' experiments were carried out in each sample in order to determine its thickness. X-ray diffraction (XRD) experiments were used for texture characterization, using a Philips PW 1710 apparatus (Cu Kα radiation). Film colour was computed from spectral data acquired using a hyperspectral imaging system. Colour specification under the standard CIE illuminant D65 was computed and represented in the CIELAB 1976 colour space [4,5]. Further detailed information can be found elsewhere [6].

Residual stresses, σ_r, were calculated from Stoney equation [7], using substrate curvature radii measurement, both before and after coating deposition [8]. Coating hardness was determined from the loading and unloading curves carried out with an ultra low load depth sensing nanoindenter—Nano instruments nanoindenter II [9], equipped with a Berkovich diamond indenter, operating at a constant displacement rate of 5 nm/s up to a constant indentation depth of 100 nm. This indentation depth was kept within the recommended value of roughly 10–20% of the film thickness [10]. Film elastic modulus was estimated by the slope of the initial portion of the unloading curve [11,12]. Hardness values were obtained from the average of 20 measurements at different positions. Ten more measurements were performed for samples showing greater dispersion.

Table 1
Thickness and composition of the samples prepared with the same bias voltage (−50 V) and variation of the gas mixture flow

Sample	Ti (at.%)	N (at.%)	O (at.%)	$\phi_{mixture}$ (sccm)	Thickness (μm)
Ti (adhesion layer)	100	–	–	–	0.3±0.1
TiN	50±3	50±3	–	$\phi_{N_2}=3.3$[a]	1.7±0.2
$TiN_{0.87}O_{0.36}$	45±3	39±3	16±3	10.0	1.1±0.1
$TiN_{0.81}O_{0.57}$	42±3	34±3	24±3	11.5	1.0±0.1
$TiN_{0.80}O_{0.63}$	41±3	33±3	26±3	12.5	1.1±0.1
$TiN_{0.69}O_{1.17}$	35±3	24±3	41±3	13.5	0.7±0.1
$TiN_{0.69}O_{1.17}$[b]	35±3	24±3	41±3	14.0	2.6±0.2
$TiN_{0.63}O_{1.23}$	35±3	22±3	43±3	14.5	0.9±0.1
$TiN_{0.69}O_{.87}$	39±3	27±3	34±3	16.0	0.9±0.1
TiO_2	33±3	–	67±3	$\phi_{O_2}=12$[a]	0.8±0.1

[a] Samples TiN and TiO_2 were prepared with a gas flux of only N_2 and O_2, respectively.
[b] Unbiased sample.

3. Results and discussion

3.1. Chemical analysis

RBS composition determination using the RUMP code simulations [13] revealed a homogenous in-depth composition for all layers [14], which is difficult to obtain in this system when comparing the high reactivity of oxygen with that of nitrogen [2]. Table 1 presents the composition and thickness of the samples.

3.2. Structure

Fig. 1 shows the XRD patterns for the TiN_xO_y samples, as well as for reference samples: titanium (adhesion layer), titanium nitride (base material) and titanium oxide. All these reference samples were prepared under the same conditions of temperature (300 °C), rotation (4 rpm), polarization of the substrate (−50 V), power (800 W) and working gas (argon) flow (100 sccm). The results reveal a strong dependence of the TiN_xO_y film texture on the oxygen content. The sample with lower percentage of this element (16 at.%)

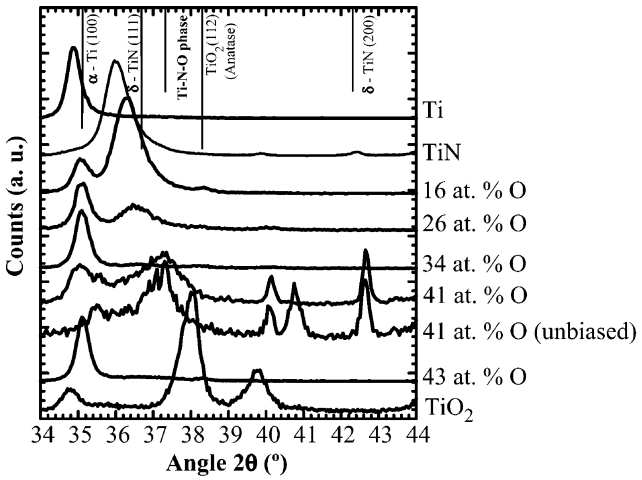

Fig. 1. Θ–2Θ XRD patterns of TiN_xO_y films with different oxygen contents.

reveals a crystalline structure, which is basically constituted by ⟨1 1 1⟩ oriented TiN grains.

The increase of the oxygen percentage is followed by a significant loss of crystallinity, being the films with the highest oxygen contents (34 and 43 at.%) practically amorphous. This amorphization of the films is related with the increase of the oxygen content promoted by the increase in the gas flow keeping in mind that oxygen is more reactive than nitrogen. The increase of the available oxygen over supersaturation level [15] reduces the possibility of crystallization (mostly that of TiN). The extended deformation of the titanium nitride structure, resulting from the incorporation of oxygen (referred here as Ti–N–O phase), increases the number of defects, and then facilitates the amorphization. This oxygen doping explains the broadening of the diffraction peaks, as it can be evidenced for intermediate and highest oxygen contents, where the peak broadening indicates the existence of microstrains and nanometer grain size. The asymmetric profile may be related to peak overlap corresponding to phase structures with different lattice parameters. In-depth structural inhomogeneities assumption may be rejected since RBS results indicate homogeneous in-depth concentrations.

Although the doping of TiN matrix with other elements has been claimed in different studies, such as those of Ti–Si–N [16] and Ti–Al–Si–N [17], the exact nature of this other phase (Ti–N–O) is somewhat difficult to evaluate, but it cannot be matched by any known compound formed with Ti and N elements, or from various phases of titanium oxide [18]. This fact provides evidence for the possible formation of an already claimed titanium, oxygen, nitrogen phase, Ti–O–N [19], where some of the oxygen atoms are most likely occupying nitrogen positions in the *fcc* TiN lattice. Without ion bombardment (Fig. 1) only the Ti–N–O phase is visible, leading to the conclusion that phase mixing is most likely a consequence of adatom mobility variations. The absence of the ion bombardment and the low deposition temperature (<300 °C) do not provide the necessary mobility for the species that will ensure the complete phase segregation, being this segregation the main reason that explains the formation of this Ti–O–N structure. Consequently, with increase in surface mobility provided by the increase in temperature and/or ion bombardment, phase segregation is enhanced and thus one can observe the formation of TiN polycrystalline grains, although traces of that Ti–O–N phase are still visible.

3.3. Colour

Fig. 2 shows the average specular colour, represented in the CIELAB 1976 colour space [4,5]. From this graph it can be seen that low oxygen contents produces a bright yellow-pink colour, which gradually shifts to dark golden yellow as the oxygen content increases. For larger contents of oxygen the colour produced is a dark blue. It is worth notice that the colour of the unbiased sample (although thicker, the colour does not change for lower thicknesses [20]) is shifted towards a white metallic ton. These results indicate that not only composition but also the phase is influencing the colour of the films. In fact these results (doped phases) revealed the possibility to produce different decorative coatings only by varying the gas flow mixture and the bias voltage, keeping constant the experimental conditions at the sputtering target.

A careful observation of the results in both graphs shows that even equal compositions can develop signif-

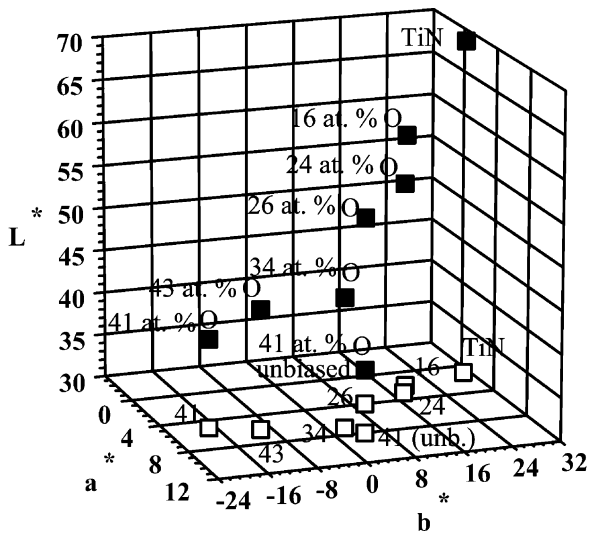

Fig. 2. Average specular colour in the CIELAB 1976 colour space for the samples under the standard CIE illuminant D_{65}. Open symbols correspond to projections in the a^*b^* plane.

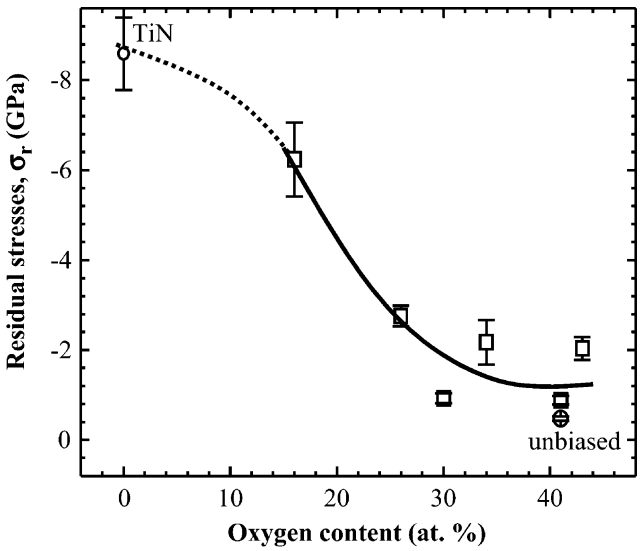

Fig. 3. Residual stresses in TiN_xO_y films as a function of the oxygen content. The lines are guides for eyes.

icantly different colours as in the case of the $TiN_{0.69}O_{1.17}$ sample. The two samples with this same composition (that prepared with 13.5 sccm gas flux and −50 V bias and that unbiased) revealed very different colours, being the negatively biased sample dark blue, while the unbiased developed a white metallic colour. Other evidences of equal compositions and very different colours can be found in other works of this group [14].

These results indicate that composition, although important, is not the main parameter that accounts for coating colour variation. Ion bombardment seems to be a much more important parameter, inducing the conclusion that the different structures and film growth conditions are influencing significantly the colour variations. The presence of the referred Ti–N–O phase is influencing significantly the coating colour. The samples with a clear TiN phase (although with traces of oxygen doped phases, seen by the peak broadening) developed a gold-brown colour, which is consistent with that of TiN. These results indicate that microstructure, influenced primarily by the preparation conditions, namely ion bombardment, is ruling the coating colour, which in turn leads to the conclusion that one can tailor this easily prepared Ti–N–O coating system with a wide variety of colours.

3.4. Mechanical characterization

3.4.1. Residual stresses

Fig. 3 shows the evolution of residual stresses as a function of the deposition parameters. From this graph it is clear that all coatings are in a compressive stress state. The unbiased sample developed also a compressive stress state, although very reduced. The explanation for this result might be in the presence of the oxygen in this sample. This element is well known for its high reactivity and thus, it is easily incorporated in the existing structures of TiN, occupying, most likely, some of the positions of nitrogen atoms. These structural defects are then responsible for the compressive stress state development, even without ion bombardment [21], such as the case of this particular sample. Regarding the evolution of the stresses with increasing oxygen content, an accentuated decrease in the value of this parameter is observed.

Though a complete fundamental understanding of the physical mechanisms involved in stress evolution is still lacking, a large set of knowledge has been assembled, some of which are summarized by Windishmann [21]. In the particular case of films prepared by sputtering, Windishmann reported on the effect of parameters such as substrate temperature, working gas pressure, working gas composition, source-to-substrate distance, substrate bias and angular distribution of adatoms. By the analysis of the published results, he suggested that for low surface mobility of adatoms, the microstructure and intrinsic stresses in a film prepared by sputtering are mostly determined by the normalized momentum delivered at the growing film, $P^*_n = \gamma(ME)^{1/2}$, where M is the mass, E is the energy and γ is the energetic particle/adatom flux ratio. P^*_n is thus a function of several deposition parameters. At high gas pressures, low temperatures and without ion bombardment during film growth, the value of P^*_n is low. The surface mobility of adatoms is thus weak and films are characterized by porous columnar microstructures [14] and the developed stresses tend to be small, lying in the region of very small compressive stresses or even tensile. At higher P^*_n the surface mobility of adatoms increases due to both the collisions with the energetic particles that arrive at the growing film, and also the larger kinetic energy of the adatoms itself. With this higher adatom mobility, voids collapse to dimensions comparable to the range of interatomic forces and the stresses tend to change from tensile to compressive. This void decrease, both in size and in number, results from the large adatom mobility, and thus the interatomic forces, which would otherwise lead to tensile stresses, are significantly reduced. Compressive stresses prevail as the film becomes denser by the so-called atomic peening effect [22].

In the case of this work, and according to Windishmann [21], the residual stress is determined mainly by the normalized moment of the particles that arrive at the film in growth. With the reduction of species mobility, resultant from the increase of the material that arrives at the film in growth (increase in the reactive gas mixture flow), the superficial mobility of deposited atoms (adatoms) is small, and thus the films developed

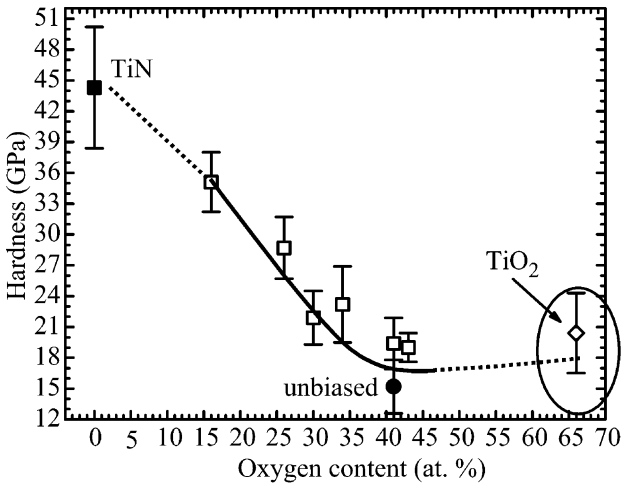

Fig. 4. Hardness and Young's modulus of sputtered TiN_xO_y films, measured by nanoindentation technique, as a function of the oxygen content. The lines are guides for the eyes.

a porous columnar growth [14] and a strong tendency for stress reduction, as in fact is observed.

Furthermore, as the percentage of oxygen increases, the distortions of the TiN crystalline lattice increase, leading to an increased tendency for film amorphization, as it can be evidenced by the diffraction patterns of Fig. 2. As a result of this increasing amorphization, the films increase their capacity to accommodate the stresses, leading to a reduction of its values. For the highest oxygen contents, the films are practically amorphous and therefore the residual stresses are very low and do not suffer significant changes.

3.4.2. Hardness

The evolution of hardness as a function of the oxygen content is illustrated in Fig. 4. The different structural changes are consistent with the hardness evolution, as it can be evidenced by the significant reduction of hardness with the increase of the oxygen content, varying from typical values of TiN films for the lowest oxygen contents, to those of TiO_2 films for the highest concentrations of this element. In this sense, it seems evident that the increase of oxygen acts as a softening factor in these coatings, and the results of both TiN and TiO_2 are consistent with the results obtained for the different oxygen contents in the TiN_xO_y films.

If it clearly seen that there is a strong dependence of the hardness on the percentage of oxygen in the films, it is also noticeable that the decrease in hardness seems to be similar to what has been reported for the variation in the residual stresses. Fig. 5 shows a plot of hardness variation with the compressive stress fields, showing a strong correlation between the film compressive stresses and hardness. Hardness increases almost linearly with increasing compressive stresses, which is believed to be due to film densification and to the presence of lattice defects in the film's structure, which acts as an obstacle for dislocation motion [23,24].

It is worth noting the case of the unbiased sample, whose hardness value is significantly lower than those of the biased samples. The absence of the ion bombardment promotes an unconstrained grain growth in this sample, which explains, not only the low stresses in this sample and the correspondent low hardening, but also large structural defects and thus low resistance to external loads. The use of a negative bias converts the porous and open columnar structures (such as that of the unbiased sample [14]) to more dense and close packed structures, increasing film hardness [6,20]. A closer look to Table 1 and Fig. 4 shows that, although the oxygen content of this unbiased sample is the same as another one prepared with −50 V bias voltage, the hardness value is relatively lower. This fact reveals that, although the oxygen content is important, it is not the only factor to take into consideration if one intends to study hardness in these Ti–N–O compounds.

A third factor that deserves some attention is the grain size. In this work, it was extremely difficult to evaluate the grain size evolution from the obtained diffraction patterns. The mixture of crystalline phases and the influence of several diffraction peaks did not allow an accurate analysis. TEM analysis in these samples is currently in progress in order to clarify the influence of this parameter. The evolution of the modulus of elasticity, illustrated in Fig. 4, follows the trend of the hardness. This type of behaviour is typical of hard and fragile materials, with brittle fracture. For such materials, the theory of Griffith [2] foresees that the hardness is proportional to the modulus of elasticity.

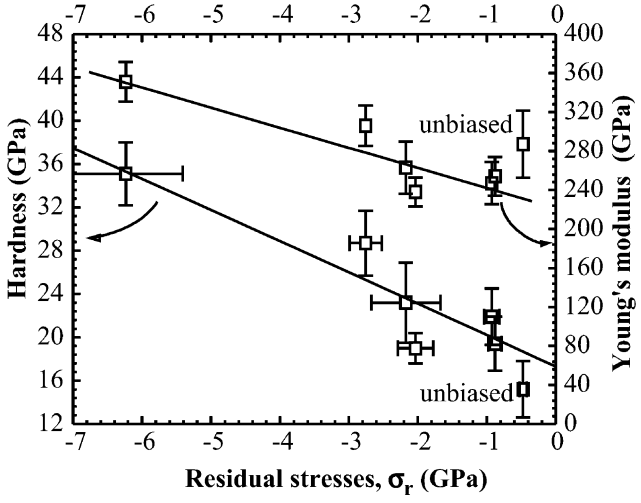

Fig. 5. Evolution of hardness vs. residual stresses in TiN_xO_y films. The lines are guides for the eyes.

4. Conclusions

Thin films within the Ti–N–O ternary system were prepared by r.f. reactive magnetron sputtering. All samples were prepared with a constant r.f. power (800 W–2.55 W/cm^2) at a Ti elemental target. Structural characterization results reveal a strong dependence of the film texture on the percentage of oxygen. The sample with lower percentage of this element (16 at.%) reveals a crystalline structure, which is basically constituted by (1 1 1) TiN grains. The increase of the oxygen percentage is followed by a significant loss in crystallinity, being the films with the highest oxygen contents amorphous. However, for intermediate and higher oxygen contents, the diffraction peaks seem to indicate a mixture of pure TiN crystalline lattice and other phases with oxygen incorporation, a Ti–N–O phase.

Regarding colour variations, it was observed that for low oxygen contents a bright yellow–pink colour was obtained, which gradually shifts to dark golden yellow as its oxygen content increases. For larger contents of oxygen the colour produced is a dark blue.

All coatings are in a compressive stress state. The unbiased sample developed also a compressive stress state, although very reduced. The increasing amorphization of the films with the increase of the oxygen content is the main parameter that seems to rule this behaviour, increasing the films' capacity to release the stresses, leading to a reduction of its values. Hardness measurements reveal a significant reduction of hardness values with the increase of the oxygen content, varying from typical values of TiN films for the lowest oxygen contents, to those of TiO_2 films for the highest concentrations of this element. The oxygen content and stresses seem to be the main parameters that explain this behaviour.

The simple method used to prepare the samples with different colours together with the relatively high hardness values and moderate compressive stresses, lead to the conclusion that one can tailor this easily prepared Ti–N–O coating system with varied colours to apply in a wide variety of decorative applications.

Acknowledgments

The authors gratefully acknowledge the financial support of the FCT institution by the project no. POCTI/CTM/380860/2001 co-financed by European community fund FEDER.

References

[1] R. Fraunchy, Surf. Sci. Rep. 38 (2000) 195, and references therein.
[2] M. Ohring, The Materials Science of Thin Films, Academic Press Inc, San Diego, 1992.
[3] C. Mitterer, J. Komenda-Stallmaier, P. Losbichler, P. Schmolz, W.S.M. Werner, H. Stori, Vacuum 46 (1995) 1281.
[4] Colorimetry, CIE Publication, 15 (1971) (Comission Internationale de L'Éclairage).
[5] Recommendations on Uniform Color Spaces, Difference–difference equations, psychometric color terms, CIE Publication, Suppl. No. 2–70 15 (1978) (Comission Internationale de L'Éclairage).
[6] F. Vaz, L. Rebouta, J.A. Mendes, S. Lanceros-Méndez, L. Cunha, S.M.C. Nascimento, Ph. Goudeau, J.P. Rivière, E. Alves, A. Sidor, Thin Solid Films 420–421 (2002) 421.
[7] G.G. Stoney, Proc. R. Soc. (Lond.) [A] 82 (1909) 172.
[8] F. Vaz, L. Rebouta, P. Goudeau, J.P. Rivière, M. Bodmann, G. Kleer, W. Döll, Thin Solid Films 402 (2002) 195, see for detailed information on the procedure.
[9] M.F. Doerner, W.D. Nix, J. Mater. Res. 1 (1992) 397.
[10] G.M. Pharr, W.C. Oliver, MRS Bull. July (1992) 28.
[11] I.N. Sneddon, Int. J. Eng. Sci. 3 (1965) 47.
[12] F. Vaz, L. Rebouta, S. Ramos, M.F. da Silva, J.C. Soares, Surf. Coat. Technol. 108–109 (1998) 236.
[13] L.R. Doolittle, Nucl. Instrum. Methods B 9 (1985) 344.
[14] F. Vaz, P. Cerqueira, L. Rebouta, S.M.C. Nascimento, E. Alves, Ph. Goudeau, J.P. Rivière, Surf. Coat. Technol. 174–175 (2003) 197.
[15] Y. Imai, M. Mukaida, A. Watanabe, T. Tsunoda, Thin Solid Films 300 (1997) 305.
[16] F. Vaz, Ph.D. Thesis, Minho University, Portugal, 2000.
[17] S. Carvalho, L. Rebouta, A. Cavaleiro, L.A. Rocha, J. Gomes, E. Alves, Thin Solid Films 398–399 (2001) 391.
[18] Powder Diffraction File of the International Center for Diffraction, PDF-ICDD 21-1272, 21-1276, and others.
[19] Powder Diffraction File of the International Center for Diffraction, PDF-ICDD Card No. 49-1325.
[20] P. Cerqueira, M.Sc. Thesis, Minho University, 2002.
[21] H. Windishmann, Crit. Rev. Solid Sate Mater. Sci. 17 (6) (1992) 547.
[22] F.M. D'Heurle, Metall. Trans. 1 (1970) 725.
[23] K. Karlsson, L. Hultman, J.-E. Sundgren, Thin Solid Films 371 (2000) 167.
[24] H. Oettel, T. Bertram, V. Weihnacht, R. Wiedemann, S.V. Zitzewitz, Surf. Coat. Technol. 97 (1997) 785.